Nano Res (2008) 1: 457–464
DOI 10.1007/s12274-008-8048-x
Research Article

InAs/InP/ZnSe Core/Shell/Shell Quantum Dots as Near-Infrared Emitters: Bright, Narrow-Band, Non-Cadmium Containing, and Biocompatible

Renguo Xie[1], Kai Chen[2], Xiaoyuan Chen[2], and Xiaogang Peng[1] (✉)

[1] Department of Chemistry and Biochemistry, University of Arkansas, Fayetteville, AR 72701, USA
[2] Molecular Imaging Program at Stanford (MIPS), Department of Radiology and Bio-X Program, Stanford University School of Medicine, Stanford, CA 94305-5484, USA

Received: 16 October 2008 / Revised: 26 October 2008 / Accepted: 26 October 2008

ABSTRACT
High quality InAs/InP/ZnSe core/shell/shell quantum dots have been grown by a one-pot approach. This engineered quantum dots with unique near-infrared (NIR) fluorescence, possessing outstanding optical properties, and the biocompatibility desired for in vivo applications. The resulting quantum dots have significantly lower intrinsic toxicity compared to NIR emissive dots containing elements such as cadmium, mercury, or lead. Also, these newly developed ultrasmall non-Cd containing and NIR-emitting quantum dots showed significantly improved circulation half-life and minimal reticuloendothelial system (RES) uptake.

KEYWORDS
Quantum dots, InAs, near-infrared (NIR), toxicity

Introduction

The use of quantum dots (QDs) for biomedical labeling is expected to be one of the first close-to-real applications of nanomaterials [1, 2]. Near-infrared (NIR) photoluminescence (PL) QDs, in particular, are likely to outperform other available biomedical labels for in vivo imaging because of their outstanding stability, large absorption cross section, and narrow emission bands [3–7]. However, NIR emitters for in vivo imaging must not only have optical performance requirements similar to their visible counterparts, but also should be small in hydrodynamic size, biocompatible, and free of extremely toxic class A elements, such as Cd, Pb, and Hg. Among all compound semiconductors, InAs-based core/shell QDs are considered one of the most feasible systems for use as NIR biomedical labels [8]. Despite the challenging synthetic chemistry of such QDs, their potential advantages have inspired continuing significant efforts [9–15] to develop high performance InAs-based NIR emitters. In general, the current challenges to overcome include low emission efficiency, broad spectrum width, poor color control, poor stability, and/or cadmium content. This work was designed to provide solutions to these problems that also offer acceptable biocompatibility for the QDs, including the necessary physiological

Address correspondence to xpeng@uark.edu

permeability, biochemical stability, negligible non-specific bonding, long circulation half-life, low cytotoxicity, and minimal reticuloendothelial system (RES) uptake.

Biological tissues are transparent in the NIR optical window (roughly between 700 and 1100 nm). Thus, if fluorescent labels can be both excited and detected efficiently in this optical window, related imaging techniques will enable imaging of live tissue without tedious isolation processes, and possibly even allow imaging directly in a biological body [16]. To fully exploit the in vivo advantages of NIR probes, the hydrodynamic size of the QDs should be less than about 10 nm and they should be stable under physiological conditions with little or no non-specific binding. Considering the thickness of the ligands, the inorganic nanocrystal core itself should be around 6–7 nm in size. Because of the well-known instability of plain core semiconductor nanocrystals, a shell with a few monolayers of wide band-gap semiconductor (commonly ZnSe or ZnS) is necessary, a requirement that further reduces the maximum size of the emissive part of the inorganic nanocrystals to below 3 nm. Among commonly known Ⅱ–Ⅵ and Ⅲ–Ⅴ semiconductors, only a select few can satisfy these requirements, such as mercury/lead chalcogenides and InAs [8]. Mercury and lead, however, are too intrinsically toxic to be considered. Although indium, arsenic, zinc, phosphorus, and selenium are also toxic, the human body can tolerate a certain level of exposure to all of these elements [8].

1. Experimental

Synthesis of InAs QDs and InAs/InP/ZnS QDs. The InAs QDs were synthesized following a procedure to be published elsewhere. The resulting InAs cores were cooled to 110 ºC. Without purification, 0.3 mmol stearic acid (in 0.5 mL octadecene (ODE)) was injected into the reaction solution, and then a mixture of 1 mmol octylamine (0.2 mL) and 0.2 mmol tris-(trimethylsilyl)phosphine ($(TMS)_3P$) in ODE (0.8 mL) was then added dropwise into the reaction solution. After addition of the P precursor, the mixture was heated to 178 ºC and the temperature maintained for 45 min in order to allow growth of the InP shell onto the InAs core. When the indium precursor had been consumed, 0.04 mmol Se in tri-*n*-octylphosphine (TOP) (0.2 mL) was injected followed by the zinc precursor zinc undecylenate. The reaction temperature was then increased to 220 ºC for 30 min to allow growth of the ZnSe shell.

Characterization of the QDs. Characterization of the QDs was carried out using a Titan microscope with an acceleration voltage of 300 kV for transmission electron microscopy (TEM) measurements, an HP 8453 diode array spectrophotometer for absorption spectra, and a Spex Fluorolog 3–111 for PL measurements.

Serum stability of QDs. InAs/InP/ZnSe QDs dispersed in 100% fetal calf serum was kept at 37 ºC. The PL intensity of the QDs in serum was measured at different times.

MTT assay of QDs. RAW 264.7 cells (mouse macrophage cell line) were seeded in a 96-well plate at a density of 5000 cells/well on the day before the addition of the QDs. InAs/InP/ZnSe QDs or QD 800 ITK carboxyl ("QD800") CdTe/ZnS core/shell dots (Invitrogen) were incubated with cells in RPMI 1640 cell culture medium in a cell culture incubator. The survival rates of the macrophage cells at 24 h and 48 h time points after dot incubation were measured by MTT assay. After 3 h incubation at 37 ºC, the MTT working solution was removed. Then 200 μL DMSO was added into each well and the plate was shaken for 20 min at room temperature. All samples were assayed in triplicate and the survival rate was calculated as follows: survival rate = $(A_{treat}/A_{control}) \times 100\%$.

In vivo and ex vivo imaging. Athymic nude mice were each injected by tail vein with 0.5 nmol of QDs. The mice were imaged at multiple time points postinjection (p.i.) using the Maestro in vivo imaging system (CRI Inc., Woburn, MA). After spectral unmixing, coronal images of multi-time points were obtained for comparison. The animals were then sacrificed at 24 h p.i. After major organs were harvested, NIR imaging was done using the IVIS 200 imaging system (Caliper Life Sciences, Hopkinton, MA).

Circulation half-life measurement. In order to measure the half-life of the InAs/InP/ZnSe QDs and Qdot 800 ITK carboxyl ("QD800") CdTe/ZnS core/shell dots (Invitrogen), nude mice were tail vein-

injected with 0.5 nmol of QDs and a blood sample (approximately 3–5 μL) was taken from the tail vein of the mice at different time points p.i. and PL intensity of the blood samples was measured by the IVIS 200 imaging system.

2. Results and discussion

The synthesis of high quality InAs core nanocrystals with the desired sizes (<3 nm) for in vivo applications has been a challenge in the field [9, 10, 13, 15]. In any case, the emission properties of InAs QDs reported so far are poor, with a weak and broad band-gap emission peak for the plain core dots. We recently developed a new synthetic strategy by applying the "self-focusing" method [17], which yielded InAs nanocrystals with their first exciton absorption peak ranging roughly from 550 nm to 1050 nm without any size sorting (Fig. 1(a)), matching the needs for NIR emitters. The outstanding properties of the InAs core nanocrystals generated by this new synthetic strategy formed the basis of this study.

The InAs core nanocrystals prepared by the new scheme showed a weak but narrow band edge PL peak without size sorting (Fig. 1(b)). After the epitaxial growth of 1–3 monolayers of an InP shell onto the InAs nanocrystals using the successive ionic layer adsorption and reaction (SILAR) technique [18] (Fig. 1(f)), the PL QY did not increase significantly, but the emission peak position could be significantly tuned by this inner shell (Fig. 1(c)). Direct epitaixal growth of ZnSe or ZnS shells onto the InAs nanocrystals improved the PL QY significantly, usually in the range of 20%–35% for ZnSe shells. Moreover, with a few monolayers of an InP buffer shell, subsequent epitaxial growth of the ZnSe shell (Fig. 1(g)) through a one-pot approach greatly improved the emissive brightness of the nanocrystals, with PL QY in the range 40%–90% (Fig. 1(d)). It should be noted that the InAs/InP/ZnSe core/shell/shell QDs have been previously reported by the Bawendi group [8]. Although the PL QY of the nanocrystals in their report was as low as 3%–5%, some interesting biomedical properties observed there provided significant inspiration for the current work.

Using our procedure, the InAs plain core and InAs/InP core/shell nanocrystals were not only dim in emission but also unstable even under ambient conditions (Fig. 2(a)). The additional epitaxial growth of the ZnSe shell, however, greatly improved the stability of the resulting nanocrystals (Fig. 2(b)). Preliminary results indicate that the InAs/InP/ZnSe/ZnSe core/shell/shell nanocrystals dissolved in nonpolar solvents did not show any signs of emission decay under ambient conditions for at least 4 months. It is also noteworthy that the InAs-based core/shell/shell QDs showed increased PL QY and improved stability only with about 2–3 monolayers of epitaxially grown ZnSe shell (Fig. 2(d)).

The PL peak width, measured by the full-width-at-half-maximum (FWHM), dictates the

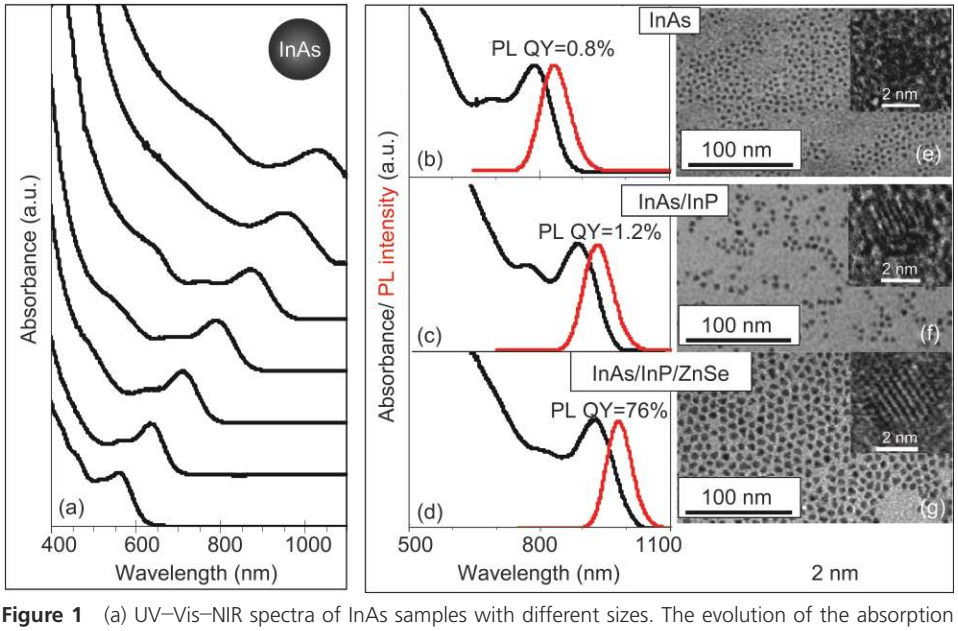

Figure 1 (a) UV–Vis–NIR spectra of InAs samples with different sizes. The evolution of the absorption and PL spectra upon consecutive growth of the concentric shells is shown in (b), (c) and (d). The spectra labeled with the letters (b)–(d) were taken from samples with TEM images as shown in (e), (f) and (g), respectively. The insets show the corresponding HR-TEM micrographs

number of possible biomedical labels within the transparent NIR window. The FWHM for the InAs core nanocrystals made by the new strategy was substantially narrower than those reported in the literature [8–10]. For example, with a UV–vis peak at around 800 nm, the PL FWHM of the InAs core nanocrystals obtained by the new strategy was about 55–65 nm (Fig. 1(b)), instead of around 100–120 nm as observed previously for the nanocrystals with a similar size and size distribution. Importantly, after growth of the InP and ZnSe shells, the PL FWHM (60–75 nm) did not change substantially (Fig. 2(c)). It should be pointed out that, given a similar size and size distribution, a narrow band gap PL peak usually indicates that the surface of the corresponding nanocrystals is more homogeneous [11, 12], which should endow the one-pot growth of the final core/shell/shell dots with outstanding qualities—substantially improved PL QY and narrower PL peak—in comparison to those reported previously that have similar structures [8].

The InAs-based QDs coated with nonpolar ligands can be readily transferred into aqueous solution by treatment with hydrophilic thiol ligands, such as mercaptopropionic acid (MPA), under basic conditions (Fig. 3(a)). Typically, the PL QY and PL peak width can be maintained on being transferred into water (Fig. 3(b)). More importantly, the resulting water-soluble nanocrystals were stable in water under ambient conditions. The hydrodynamic sizes of the InAs-based QDs in water were controlled to be below 10 nm.

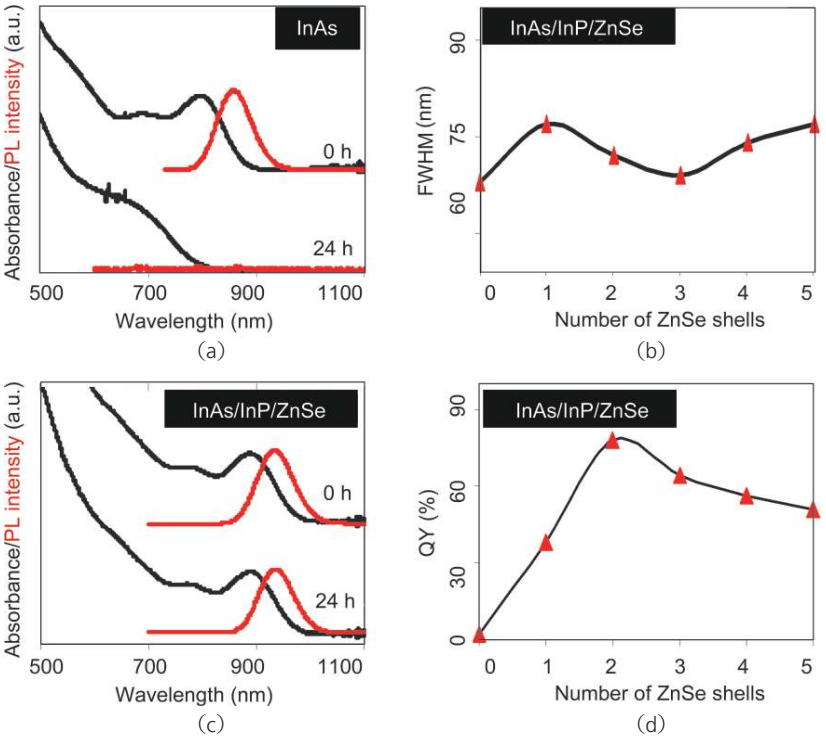

Figure 2 Air stability of (a) InAs and (b) InAs/InP/ZnSe core/shell dots. The evolution of PL FWHM and PL QY of InAs/InP/ZnSe core/shell dots with different ZnSe shells is shown in (c) and (d)

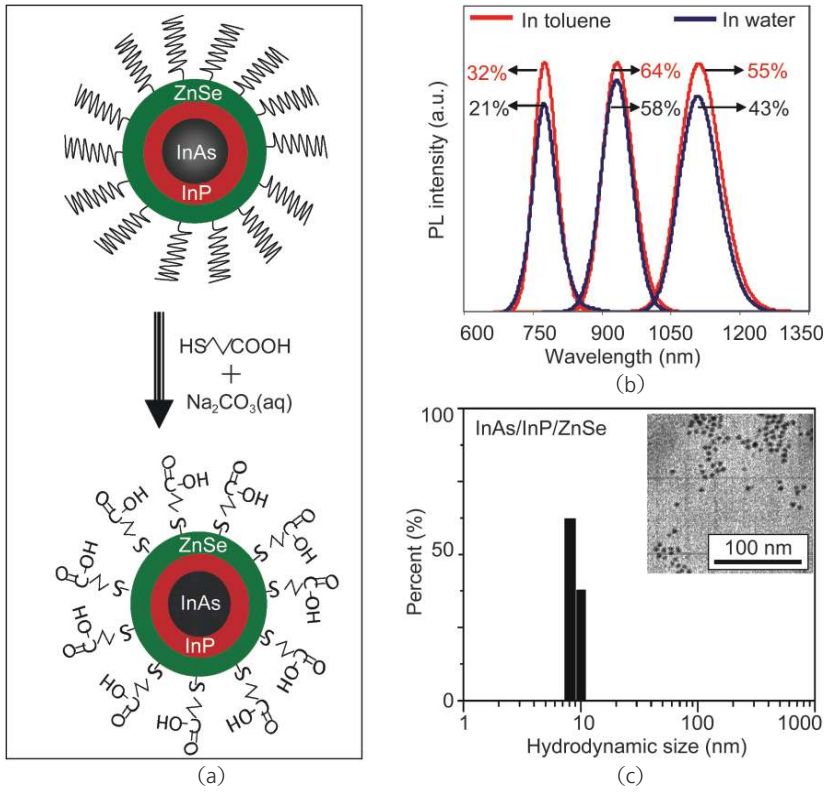

Figure 3 (a) Schematic representation of ligand exchange process to prepare core/shell/shell dots using MPA; (b) the QY of as-obtained three core/shell/shell dots dispersed first in toluene and then in water; (c) dynamic light scattering measurements of the hydrodynamic diameter of exchanged core/shell/shell dots with MPA in water. Inset is the TEM image of core/shell /shell quantum dots in water

The example in Fig. 3(c), with its PL peak position at 940 nm, was determined to have average diameter of about 8–9 nm by dynamic light scattering. This hydrodynamic size approximately matched the size estimated from the physical dimensions of the nanocrystals i.e., a ~6 nm inorganic nanocrystal with a ~1.4 nm ligand shell. By TEM, these water-soluble QDs were found be well separated as individual dots (Fig. 3(c), inset).

The results above demonstrate that the InAs-based QDs presented here are extremely bright, chemically stable, tunable in emission color in the targeted NIR window, and below the requisite 10 nm size threshold for in vivo applications in water. To examine the biostability of the water-soluble InAs/InP/ZnSe core/shell/shell dots, they were mixed with pure serum obtained from commercial sources. Figure 4 shows that the emission properties of the dots did not change after mixing with the serum. After removing the significant scattering background caused by the large particles in serum (dashed line in Fig. 4(a)), the absorption spectrum (not shown) of the InAs/InP/ZnSe core/shell/shell dots in serum was essentially the same as that of the dots in water (Fig. 4(b)). Figure 4(c) indicates that, despite the strong scattering and absorption by the serum medium (barely transparent), the deep red emission of the core/shell sample was nearly the same as that of the dots in pure water. This is consistent with the transparent features of the biological system in the deep red and the NIR window mentioned above. Upon incubation in the serum under typical body temperature (37 °C) for at least 2 days, the emission properties of the InAs/InP/ZnSe core/shell/shell dots were found to remain unchanged. These results clearly indicate no noticeable aggregation of the dots under the physiological conditions employed.

We conducted some preliminary studies on the non-specific bonding of InAs/InP/ZnSe core/shell/shell dots onto biological species in serum. This was performed by high-speed centrifugation (14 000 rpm) of the incubated mixture of the dots and serum (incubated for 1 day at 37 °C). The picture in Fig. 4(e) (left) illustrates the strong scattering of the mixture caused by the biomolecule suspensions in serum before centrifugation. As a result, the letters "InAs NCs" behind the cuvette were barely visible. Upon centrifugation, the supernatant became optically clear, which made it possible to see the letters "InAs NCs" behind the optical cuvette (Fig. 4(e), right).

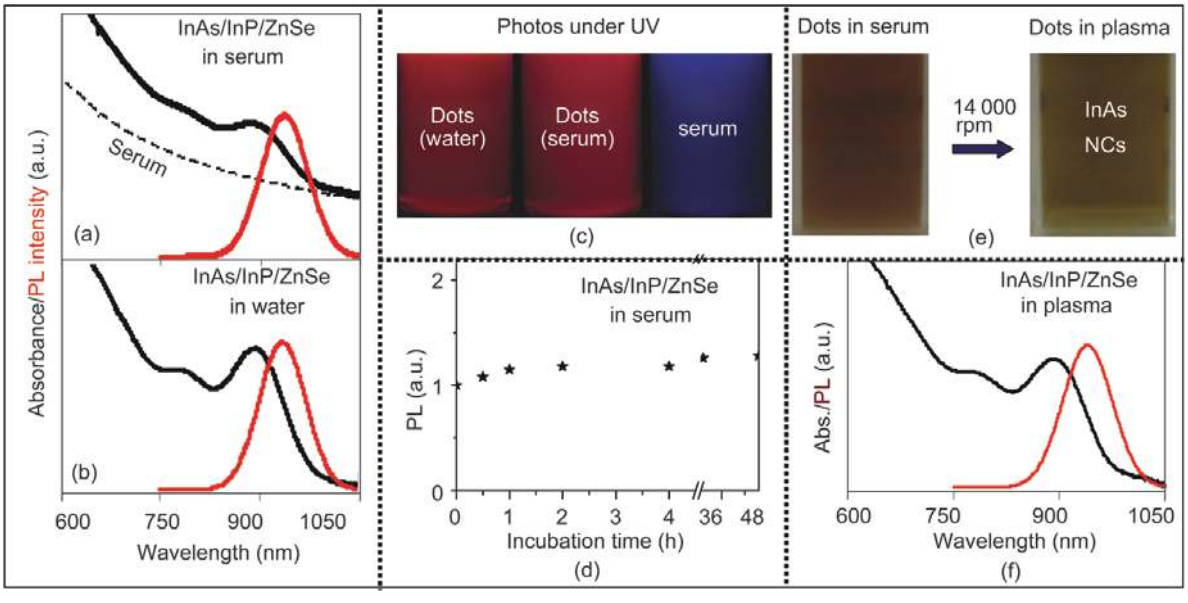

Figure 4 UV–vis–NIR and PL spectra of core/shell/shell dots in (a) serum and (b) water; (c) digital pictures of core/shell/shell dots in water and serum, and pure serum under UV light; (d) PL intensity of the core/shell/shell dots recorded over 2 days of incubation in serum at 37 °C; (e) digital pictures of core/shell/shell nanocrystal sample in serum before and after centrifugation; (f) UV–vis–NIR and PL spectra of the supernatant of the sample in (e)

This means that most of the scattering biomolecules were successfully removed by the centrifugation process. The optical properties of the InAs/InP/ZnSe core/shell/shell dots in the supernatant (Fig. 4(f)), however, showed identical absorbance and PL emission intensity. This indicates that the non-specific bonding of the InAs/InP/ZnSe core/shell/shell dots to large-sized biomolecules present in the serum was negligible, if present at all. This interesting phenomenon and the non-aggregation features of the dots in the serum are positive proof of the potential for in vivo biomedical applications of the dots. Although the exact mechanism(s) underlying the encouraging results in Fig. 4 needs further clarification, some preliminary biomedical tests to be discussed below further confirmed the excellent performance of the InAs/InP/ZnSe core/shell/shell dots for biomedical labeling (Fig. 5).

To further explore the potential in vivo applications of InAs/InP/ZnSe core/shell/shell dots, we studied their cytotoxicity in vitro, circulation half-life, and major organ distribution in vivo. The results were compared with a standard commercial product with its PL in the similar NIR window, QD 800 ITK carboxyl ("QD800") CdTe/ZnS core/shell dots (Invitrogen). MTT assay (Fig. 5(a)) revealed significantly less cytotoxicity of InAs/InP/ZnSe core/shell/shell dots as compared to CdTe/ZnS core/shell dots. When incubated with RAW 264.7 mouse macrophage cells, QD800 had significantly higher cell uptake and retention than InAs/InP/ZnSe core/shell/shell dots (data not shown). Non-invasive fluorescence imaging (Fig. 5(b)) revealed significantly higher and more prolonged liver uptake

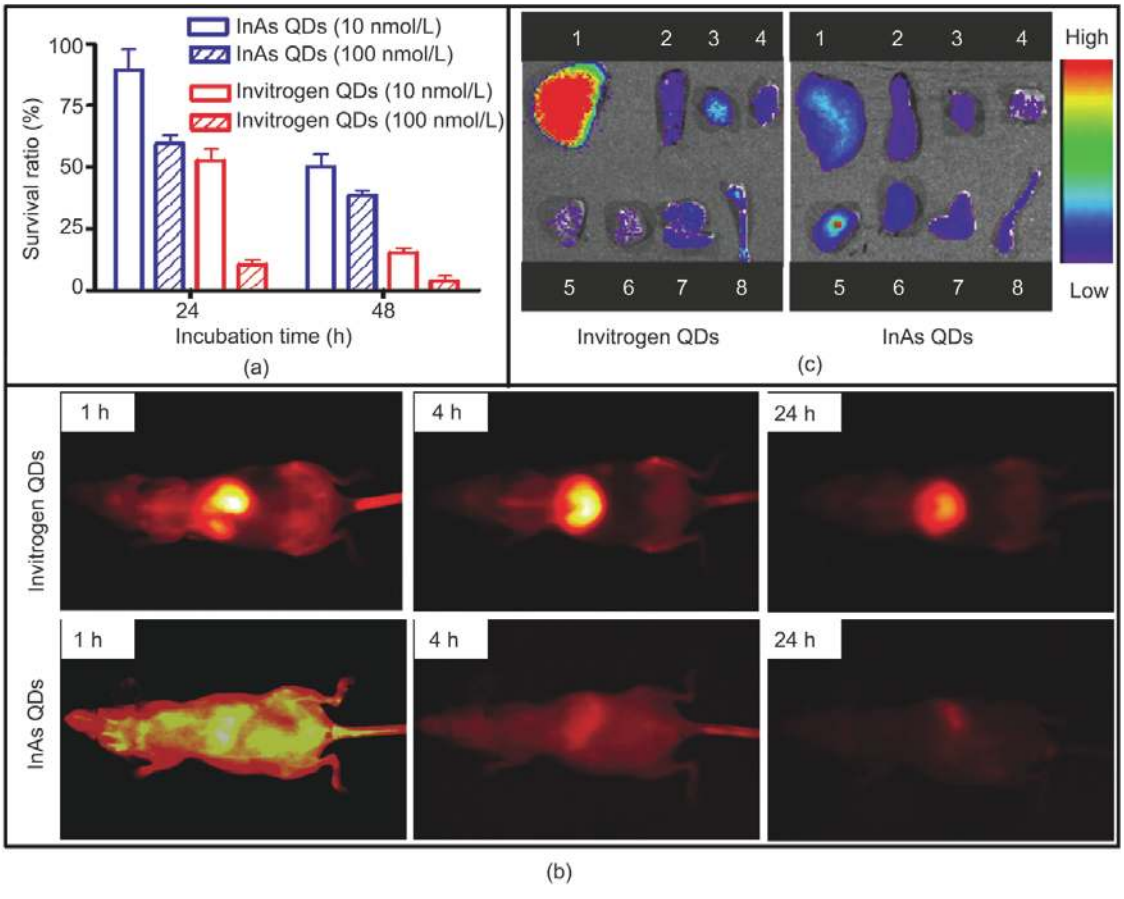

Figure 5 In vitro and in vivo characterization of quantum dots: (a) In vitro toxicity of quantum dots measured by MTT assay using mouse macrophage cell line RAW 264.7; (b) in vivo NIR fluorescence imaging of athymic nude mice injected with 0.5 nmol of InAs/InP/ZnSe core/shell/shell dots (bottom) and Invitrogen Qdot 800 ITK carboxyl ("QD800") CdTe/ZnS core/shell dots (top); (c) ex vivo fluorescence imaging of major organs of mice at 24 h post injection: 1, liver; 2, spleen; 3, heart; 4, muscle; 5, left kidney; 6, right kidney; 7, lung; 8, bone

for the CdTe/ZnS core/shell dots. In the meantime, mice urine was collected at 1 h post injection and fluorescence intensity was measured. After normalization by quantum yield and injection dose, the percentage of urine clearance of InAs/InP/ZnSe core/shell/shell dots was 0.033%/μL. The amount of InAs/InP/ZnSe core/shell/shell dots was 2.79 times the amount of CdTe/ZnS core/shell dots, which strongly indicated renal clearance of InAs/InP/ZnSe core/shell/shell dots. Ex vivo imaging of major organs and tissues at 24 h after intravenous injection of QDs (Fig. 5(c)) confirmed much lower liver signals from mice injected with InAs/InP/ZnSe core/shell/shell dots than those injected with CdTe/ZnS core/shell dots. The higher signals from the kidneys of mice injected with InAs/InP/ZnSe core/shell/shell dots suggest renal clearance of this type of non-cadmium-based QDs.

The decrease in fluorescence signals of both particles in the blood circulation was followed by one-phase exponential decay with the circulation half-life for InAs/InP/ZnSe core/shell/shell dots being as long as 110 min, whereas the half-life for CdTe/ZnS core/shell dots was only 6 min. The short circulation half-life of CdTe/ZnS core/shell dots measured from fluorescence spectrometry is consistent with our previous results reported in the literature [19, 20].

3. Conclusions

InAs/InP/ZnSe core/shell/shell dots grown by the one-pot approach can be engineered as unique NIR fluorescence labels that possess outstanding optical properties and the biocompatibility desired for in vivo applications. Although the dots still contain different types of toxic elements such as In, As, P, Zn, and Se, the intrinsic toxicity of the resulting dots is significantly reduced compared to NIR emissive dots containing cadmium, mercury, or lead. These potential labels have higher brightness, higher molar extinction coefficient, broader absorption bands covering an optical window from NIR to UV, and sharper PL peaks in the NIR window than NIR-emitting organic dyes and/or existing QDs. The hydrodynamic sizes of the resulting bright NIR core/shell/shell dots in water can be controlled to be below the required 10 nm threshold. These water-soluble InAs/InP/ZnSe core/shell/shell dots were found not to aggregate under physiological conditions tested, and their non-specific bonding to large sized biomolecules was insignificant. Finally, these newly developed ultrasmall non-Cd and NIR-emitting QDs showed significantly improved circulation half-life and minimal RES uptake. With such unique and desirable properties, these high-performance NIR emission dots should offer a new, attractive platform for exploring biomedical labeling using colloidal QDs, especially for in vivo molecular imaging applications.

Acknowledgements

This work was supported in part by the National Cancer Institute (NCI) (R21 CA121842, P50 CA114747, and U54 CA119367), the National Institute of Health (R43 EB005072), and the National Science Foundation (CHE-0554812).

References

[1] Bruchez, M., Jr.; Moronne, M.; Gin, P.; Weiss, S.; Alivisatos, A. P. Semiconductor nanocrystals as fluorescent biological labels. *Science* **1998**, *281*, 2013–2016.

[2] Chan, W. C. W.; Nie, S. M. Quantum dot bioconjugates for ultrasensitive nonisotopic detection. *Science* **1998**, *281*, 2016–2018.

[3] Dubertret, B.; Skourides, P.; Norris, D. J.; Noireaux, V; Brivanlou, A. H.; Libchaber, A. In vivo imaging of quantum dots encapsulated in phospholipid micelles. *Science* **2002**, *298*, 1759–1762.

[4] Larson, D. R.; Zipfel, W. R.; Williams, R. M.; Clark, S. W.; Bruchez, M. P.; Wise, F. W.; Webb, W. W. Water-soluble quantum dots for multiphoton fluorescence imaging in vivo. *Science* **2003**, *300*, 1434–1436.

[5] Kim, S.; Lim, Y. T.; Soltesz, E. G.; De Grand, A. M.; Lee, J.; Nakayama, A.; Parker, J. A.; Mihaljevic, T.; Laurence, R. G.; Dor, D. M.; Cohn, L. H.; Bawendi, M. G.; Frangioni, J. V. Near-infrared fluorescent type II quantum dots for sentinel lymph node mapping. *Nat. Biotechnol.* **2004**, *22*, 93–97.

[6] Gao, X. H.; Cui, Y. Y.; Levenson, R. M.; Chung, L. W. K.; Nie, S. M. In vivo cancer targeting and imaging with semiconductor quantum dots. *Nat*. *Biotechnol*. **2004**, *22*, 969–976.

[7] Michalet, X.; Pinaud, F. F.; Bentolila, L. A.; Tsay, J. M.; Doose, S.; Li, J. J.; Sundarensan, G.; Wu, A. M.; Gambhir, S. S.; Weiss, S. Quantum dots for live cells, in vivo imaging, and diagnostics. *Science* **2005**, *307*, 538–544.

[8] Zimmer, J. P.; Kim, S. W.; Ohnishi, S.; Tanaka, E.; Frangioni, J. V.; Bawendi, M. G. Size series of small indium arsenide-zinc selenide core-shell nanocrystals and their application to in vivo imaging. *J. Am. Chem. Soc*. **2006**, *128*, 2526–2527.

[9] Guzelian, A. A.; Banin, U.; Kadavanich, A. V.; Peng, X.; Alivisatos, A. P. Colloidal chemical synthesis and characterization of InAs nanocrystal quantum dots. *Appl. Phys. Lett*. **1996**, *69*, 1432–1434.

[10] Cao, Y. W.; Banin, U. Synthesis and characterization of InAs/InP and InAs/CdSe core/shell nanocrystals. *Angew. Chem. Int. Ed*. **1999**, *38*, 3692–3694.

[11] Qu, L.H.; Peng, X. G. Control of photoluminescence properties of CdSe nanocrystals in growth. *J. Am. Chem. Soc*. **2002**, *124*, 2049–2055.

[12] Talapin, D. V.; Rogach, A. L.; Shevchenko, E. V.; Kornowski, A.; Haase, M.; Weller, H. Dynamic distribution of growth rates within the ensembles of colloidal II–VI and III–V semiconductor nanocrystals as a factor governing their photoluminescence efficiency. *J. Am. Chem. Soc*. **2002**, *124*, 5782–5790.

[13] Battaglia, D.; Peng. X. G. Formation of high quality InP and InAs nanocrystals in a noncoordinating solvent. *Nano Lett*. **2002**, *2*, 1027–1030.

[14] Yu, P. R.; Beard, M. C.; Ellingson, R. J.; Ferrere, S.; Curtis, C.; Drexler, J.; Luiszer, F.; Nozik, A. J. Absorption cross-section and related optical properties of colloidal InAs quantum dots. *J. Phys. Chem. B* **2005**, *109*, 7084–7087.

[15] Aharoni, A.; Mokari, T.; Popov, I.; Banin, U. Synthesis of InAs/CdSe/ZnSe core/shell/shell structures with bright and stable near-infrared fluorescence. *J. Am. Chem. Soc*. **2006**, *128*, 257–264.

[16] Cai, W. B.; Shin, D. W.; Chen, K.; Gheysens, O.; Cao, Q. Z.; Wang, S. X.; Gambhir, S. S.; Chen, X, Y. Peptide-labeled near-infrared quantum dots for imaging tumor vasculature in living subjects. *Nano Lett*. **2006**, *6*, 669–676.

[17] Xie, R.G.; Peng, X. G. Synthetic scheme for high-quality InAs nanocrystals based on self-focusing and one-pot synthesis of InAs-based core-shell nanocrystals. *Angew. Chem. Int. Ed*. **2008**, *47*, 7677–7680.

[18] Li, J. J.; Wang, A.; Guo, W. Z.; Keay, J. C.; Mishima, T. D.; Johnson, M. B.; Peng, X. G. Large-scale synthesis of nearly monodisperse CdSe/CdS core/shell nanocrystals using air-stable reagents via successive ion layer adsorption and reaction. *J. Am. Chem. Soc*. **2003**, *125*, 12567–12575.

[19] Schipper, M. L.; Cheng, Z.; Lee, S. W.; Bentolila, L. A.; Iyer, G.; Rao, J, H.; Chen, X. Y.; Wu, A. M.; Weiss, S.; Gambhir, S. S. Micro PET-based biodistribution of quantum dots in living mice. *J. Nucl. Med*. **2007**, *48*, 1511–1518.

[20] Sun, X. M. ; Liu, Z.; Welsher, K.; Robinson, J. T.; Goodwin, A.; Zaric, S.; Dai, H. J. Nano-graphene oxide for cellular imaging and drug delivery. *Nano Res*. **2008**, *1*, 203–212.